European Heart Journal – Cardiovascular Imaging (2012) **13**, 370–384
doi:10.1093/ehjci/jes025

REVIEW

Optical coherence tomography: from research to practice

Juan Luis Gutiérrez-Chico[1], Eduardo Alegría-Barrero[2], Rodrigo Teijeiro-Mestre[2], Pak Hei Chan[2], Hiroto Tsujioka[3], Ranil de Silva[2], Nicola Viceconte[2], Alistair Lindsay[2], Tiffany Patterson[2], Nicolas Foin[4], Takashi Akasaka[3], and Carlo di Mario[2,4]*

[1]Institute for Cardiovascular Translational Research of the Atlantic, Vigo (Pontevedra), Spain; [2]Cardiovascular Biomedical Research Unit, Royal Brompton and Harefield NHS Foundation Trust, Sydney Street, London SW3 6NP, UK; [3]Wakayama Medical University, Wakayama, Japan; and [4]Imperial College of London, London, UK

Received 10 October 2011; accepted after revision 11 January 2012; online publish-ahead-of-print 13 February 2012

Optical coherence tomography (OCT) is a high-resolution imaging technique with great versatility of applications. In cardiology, OCT has remained hitherto as a research tool for characterization of vulnerable plaques and evaluation of neointimal healing after stenting. However, OCT is now successfully applied in different clinical scenarios, and the introduction of frequency domain analysis simplified its application to the point it can be considered a potential alternative to intravascular ultrasound for clinical decision-making in some cases. This article reviews the use of OCT for assessment of lesion severity, characterization of acute coronary syndromes, guidance of intracoronary stenting, and evaluation of long-term results.

Keywords Atherosclerotic plaque • Optical coherence tomography • Intravascular imaging • Stent • Apposition • Neointima • Intimal hyperplasia

Introduction

Coronary angiography is the workhorse invasive imaging technique for diagnostic and interventional procedures. The simple injection of a radiopaque contrast medium provides an accurate real-time luminogram, which can translate into accurate and highly reproducible measurements for clinical decision-making and for research applications.[1,2] However, angiography looses accuracy in the presence of overlapping vessels, foreshortening, or calcium in the vessel wall. Furthermore, angiography has limited ability to characterize tissue and atherosclerotic plaques, beyond the detection of calcium and grossly ulcerated plaques or dissections. Thus, there are some scenarios in which an experienced interventional cardiologist requires complementary information to that provided by angiography.

Intravascular ultrasound (IVUS) can improve the accuracy of the coronary luminogram in cases of overlapping, foreshortened or calcified vessels, imaging also the vessel wall, and giving information about the plaque burden, plaque morphology, or calcium distribution. Optical coherence tomography (OCT) uses near-infrared light (NIR) to generate cross-sectional images of the coronary arteries. NIR has shorter wavelength and higher frequency than ultrasound; therefore, OCT images have 10-fold higher resolution than IVUS images, at the expense of lower penetration into the tissue. The higher resolution of OCT enables the visualization and measurement of details that had remained elusive for angiography and IVUS hitherto, whereas its lower tissue penetration determines most of OCT limitations (*Table 1*). Although OCT started in cardiology as a research tool, it has the potential to become a routine tool for diagnostic application and guidance of therapeutic interventions. This article analyses advantages and limitations of OCT compared with other intravascular imaging methods for a widespread array of clinical applications such as assessment of lesion severity, characterization of acute coronary syndromes (ACS), guidance of intracoronary stenting, and evaluation of long-term healing post-stenting.

Lesion assessment pre-intervention

Assessment of lesion severity

Previous studies have shown that OCT can study coronary plaque morphology and identify thrombus, intimal rupture, lipid-laden

* Corresponding author. Tel/fax: +44 20 7352 8121, Email: c.dimario@rbht.nhs.uk

Table 1 Comparative technical summary of the three main imaging modalities used in interventional cardiology for diagnostic and for interventional purposes

	Angiography	IVUS	OCT
Radiation type	X-radiation	Ultrasound	NIR light
Frequency	3×10^3–3×10^7THz	20–45 MHz	192 THz
Wavelength (μm)	10^{-5}–10^{-2}	35–80	1.3
Axial resolution (μm)	59–137	100–200	10–20
Lateral resolution (μm)	NA	200–300	20–90
Rotation speed (Hz)	NA	30	16–160
Pull-back speed (mm/s)	NA	0.5–1	1–20
Tissue penetration (mm)	200–450	10	1–3
Scan diameter—field of view (mm)	NA	15	7–11
Usefulness for			
Plaque/tissue characterization	+	++	+++
Expansion/sizing	+	+++	+++
Apposition	−	++	+++
Vascular injury	+	++	+++
Intervention guidance	++	+	+
Assessment of restenosis/NIH	+++	+++	++
Assessment of coverage	−	−	+++

The usefulness of each imaging technique for different applications has been graded from 'not useful' (−) to 'very useful' (+++), according to the rationale explained in the text. IVUS, intravascular ultrasound; NA, not applicable; NIH, neointimal hyperplasia; OCT, optical coherence tomography.

plaques, and thickness of the fibrous cap. Potentially, OCT also provides accurate quantitative measurements that can guide clinicians to decide whether a coronary lesion deserves treatment.

Different observational studies validated IVUS for the assessment of lesion severity[3–5] An absolute minimal lumen cross-sectional area (MLCSA) of $<4\ mm^2$ was strongly correlated with a fractional flow reserve (FFR) of <0.75,[4] with a coronary flow reserve of <2,[3] or with perfusion defects in single-photon emission computed tomography.[5] More recent studies have questioned these findings and the concept of using absolute MLCSA for the assessment of lesion severity.[6–8] FFR has the intrinsic advantage of providing a cut-off value independent of the vessel size, with solid evidence linking results and clinical outcome.[9,10] When larger studies compared IVUS MLCSA, and FFR, the cut-off values were lower than those traditionally accepted.[7,8]

OCT has been validated *in vitro* and *in vivo* for lumen measurements, demonstrating higher accuracy[11,12] and reproducibility[13] than IVUS. However, and contrary to IVUS, OCT has not been validated for the assessment of functional severity in coronary stenosis hitherto. There are no studies comparing FFR and OCT MLCSA, although they would be interesting for several reasons: IVUS consistently overestimates lumen areas with respect to OCT[11,14]; therefore, the eventual cut-off values would be probably different. OCT can be of particular advantage for intermediate in-stent restenosis (*Figure 1*) because the very soft neointimal plaque can sometimes be missed by IVUS and because OCT can unravel as well as IVUS the prevalent mechanism of restenosis (incomplete expansion vs. intimal proliferation) due to the ability to visualize struts deep in the vessel wall taking advantage of the powerful optical reflectance of the stent struts.

Optical coherence tomography in acute coronary syndromes

Patients hospitalized with ACS remain at high risk of adverse events, with a reported rate of death or non-fatal myocardial infarction of 15.8% at 6 months.[15] *In vivo* investigation of coronary plaque morphology may provide insights into mechanisms leading to ACS and may facilitate the identification of coronary lesions and patients who may be at risk of a future ACS. A number of intracoronary imaging modalities have assessed coronary plaque morphology in patients with ACS[16] and their prognostic significance.[17] The high spatial resolution of OCT enables identification of coronary plaque features previously undetectable for conventional intracoronary imaging methods. This may contribute to a better understanding of the pathophysiology of ACS and lead to the development of management strategies aimed at reducing the risk of future adverse events.

OCT allows high-resolution interrogation of atherosclerotic coronary plaques *in vivo*, based on validated measurements of vessel wall and lumen dimensions[18,19] and characterization of plaque constituents.[20–23] The first clinical use of intracoronary OCT using a prototype system demonstrated the differential prevalence of thin cap fibroatheroma (*Figure 2*) in patients with acute ST elevation ACS (STEACS) (72%), non-ST elevation ACS (NSTEACS) (50%), and stable angina pectoris (SAP) (20%).[24] More recently, Kubo *et al.*[25] showed the presence of plaque rupture in 73% of the patients with acute STEACS, which was only detectable in 47 and 40% of cases by angioscopy and IVUS, respectively. Thin-capped fibroatheroma (TCFA) was observed in 83% of the cases by OCT as the underlying plaque morphology. Furthermore, these investigators demonstrated that the sensitivity of IVUS to detect thrombus was only 33%, raising to 100% for OCT. Finally, OCT identified plaque erosion in 23% of the cases in which IVUS and angioscopy failed to detect it.[25] These early *in vivo* data were consistent with previous histopathological assessments of coronary plaque morphology and mechanism of plaque instability in patients after sudden cardiac deaths presumed secondary to ACS[26,27] and demonstrate the superiority of OCT over other conventional intracoronary imaging modalities for plaque characterization in patients with ACS.[25]

Following these initial reports, a number of investigators have exploited the exquisite resolution of OCT to obtain new mechanistic insights into the development of ACS[24,25,28–33] (*Table 2*). Studies in the culprit arteries of patients with STEACS have demonstrated the presence of plaque rupture in 25–77%, intraluminal thrombus in 20–100% of the cases, and TCFA in 51–85% of the cases.[24,28,31–33] While some studies reported

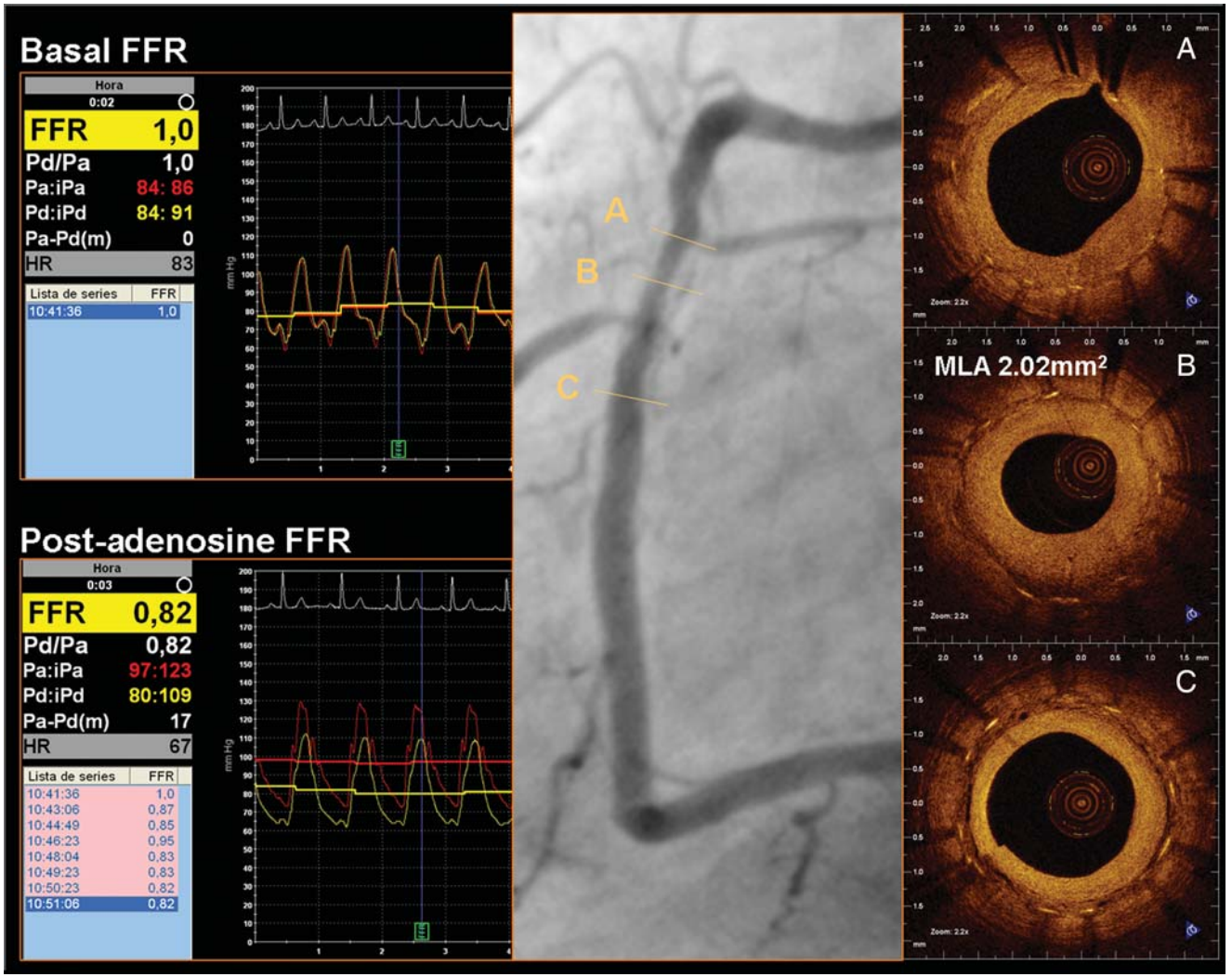

Figure 1 A 51-year-old male with non-ST-segment elevation myocardial infarction was treated with implantation of a bare-metal stent. Six months later, the patient complained of exertional Canadian Cardiovascular Class II angina. Single-photon emission computed tomography showed an inferior perfusion defect after exercise. Optical coherence tomography showed severe restenosis of the stent, with predominantly homogeneous density, compatible with fibrous tissue, low peri-strut density, and rich microvasculature around the struts. The point of minimum lumen area (MLA) was 2.02 mm^2. (B) Fractional flow reserve, however, was 1.0 at basal conditions and 0.82 after maximal vasodilation. The optimal treatment of this case remains controversial.

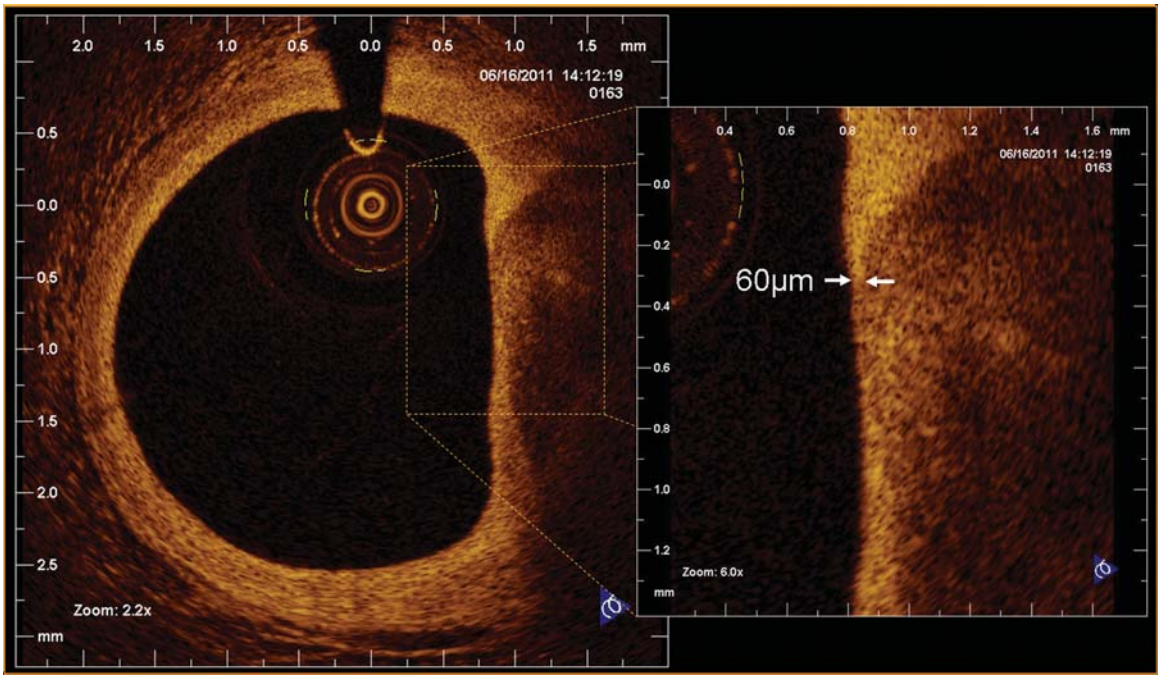

Figure 2 Thin-capped fibroatheroma in optical coherence tomography, defined as a plaque with lipid content in two or more quadrants and thickness of the fibrous cap $\leq$65 µm.

a prevalence of plaque rupture and thrombus similar to those in postmortem examinations,[31,33] others have reported lower frequencies of these features in patients with STEACS.[24,28,32] This discrepancy may be due to the timing of the OCT study, prior use of thrombolysis and/or glycoprotein IIb/IIIa inhibitor, and heavy thrombus burden, which may obscure the underlying plaque.

While these initial studies have suggested that plaque rupture of a TCFA is a major mechanism underlying ACS, several recent reports have raised important new questions. First, recent data suggest that ruptured plaques in ACS had thicker fibrous caps if the angina was exertion-triggered than when symptoms occurred at rest.[34] Plaque rupture is considered the main mechanism of both STEACS and NSTEACS. The superior resolution of OCT offers insight into potential subtle differences in the pathological changes underlying these two ACS. Ino *et al.* performed OCT studies in patients with both STEACS and NSTEACS and showed that the prevalence of TCFA, plaque rupture, and thrombus were lower in patients with NSTEACS.[33] These investigators also showed that the sites of plaque rupture were differentially located with respect to the direction of blood flow, with the majority of rupture sites in the STEACS population occurring upstream.[33] Furthermore, it is clear that TCFA can be observed in both the culprit and non-culprit arteries of patients with ACS[28] as well as patients with stable coronary disease.[24,28,29,31] These investigators have also shown that TCFAs were observed to cluster in the proximal LAD, but were more evenly distributed throughout the left circumflex artery and right coronary artery,[35] consistent with previous histopathological reports.[36] Plaque morphology alone may be insufficient to identify lesions at risk of becoming unstable, as in prospective studies, many plaques with these apparently 'high-risk' morphological features remain clinically silent.[28]

Assessment of intracoronary devices

Assessment during stent implantation

The widespread application of a non-occlusive technique using monorail OCT catheters and the high pull-back speed (up to 20 mm/s) allowed by newer generation FD-OCT systems revived the interest in OCT for procedural guidance of coronary interventions. Automatic measurement of lumen values helps to take decisions in a timely fashion. The additional contrast dose required for OCT acquisition is a potential drawback, but this amount can be minimized by expert operators using it only in key steps once an angiographic optimisation has been already achieved. Arrhythmias and chest discomfort caused in the past by the need of transient proximal balloon occlusion and of a prolonged selective contrast injection are not anymore of concern using a non-occlusive technique and the fast pull-back of FD-OCT.[37]

Before stenting, OCT provides a wealth of information on lesion characteristics such as the presence and type of thrombus, TCFA, plaque ulceration, or superficial calcification that can help to guide the procedure, suggesting the need for ancillary devices or for dedicated stents (e.g. covered stents). For cases of in-stent restenosis, OCT provides information on the degree and localization of neointimal hyperplasia and on the stent area. For complex

Table 2 Optical coherence tomographic findings in culprit and non-culprit lesion from *in vivo* observational studies

Reference	Population	Plaque rupture	Intracoronary thrombosis	TCFA	Fibrous cap thickness (μm)	Time to OCT imaging
Jang *et al.*[24]	$n = 20$, STEACS	STEACS 25%	STEACS 20%	STEACS 72%	STEACS 47	STEACS 4.6 ± 5.3 days
	$n = 20$, NSTEACS	NSTEACS 15%	NSTEACS 25%	NSTEACS 52%	NSTEACS 53.8	NSTEACS 3.3 + 1.7 days
	$n = 17$, SAP	SAP 12%	SAP 35%	SAP 20%	SAP 102.6	SAP —
Kubo *et al.*[25]	$n = 30$, STEACS	73%	100%	83%	49 ± 21	3.8 ± 1.0 h
Fujii *et al.*[28]	$n = 35$, STEACS; $n = 20$, SAP; 3-vessel study	STEACS Culprit 46% Non-culprit 31%; SAP Culprit 10% Non-culprit 15%	STEACS Culprit 95% Non-culprit 45%; SAP Culprit 25% Non-culprit 15%	STEACS Culprit 77% Non-culprit 77%; SAP Culprit 25% Non-culprit 30%	—	—
Sawada *et al.*[29]	$n = 129$, SAP, plaques in culprit artery	—	—	29%	—	—
Tanaka *et al.*[30]	$n = 83$, NSTEACS	52%	82%	22%	—	29 ± 26 h
Kubo *et al.*[31]	$n = 26$, STEACS	STEACS 77%	STEACS 100%	STEACS 85%	STEACS 57 ± 12	STEACS 4.4 ± 1.2 h
	$n = 16$, SAP	SAP 7%	SAP 0%	SAP 13%	SAP 180 ± 65	SAP —
Toutouzas *et al.*[32]	$n = 55$, STEACS	49%	65%	51%	NS	3.08 ± 0.97 h
Ino *et al.*[33]	$n = 40$, STEACS	STEACS 70%	STEACS 78%	STEACS 78%	STEACS 55 ± 20	STEACS 3.9 h
	$n = 49$, NSTEACS	NSTEACS 47%	NSTEACS 49%	NSTEACS 27%	NSTEACS 109 ± 55	NSTEACS 14.5 h

NS, not specified; NSTEACS, non-ST-segment elevation acute coronary syndrome; OCT, optical coherence tomography; SAP, stable angina pectoris; STEACS, ST-segment elevation acute coronary syndrome; TCFA, thin-capped fibroatheroma.

procedures, like after recanalization of chronic total occlusions (*Figure 3*), OCT can orientate about the extent of calcific and fibrotic changes and detect the presence of subintimal wire positions, distal dissections, or double channels potentially useful to determine the length of the segment to stent. Although there is general consensus about the ability of OCT to provide detailed information potentially useful to guide the intervention, there is currently no evidence that an OCT-guided percutaneous coronary intervention (PCI) has any advantage over conventional IVUS or angiographic guidance.

For OCT, the selection of balloon diameter is most often based on the lumen rather than on the vessel area/diameter. The initial criteria proposed by Colombo and colleagues[38] for IVUS were based on a combination of vessel and lumen area/diameter, and the Milan group has recently proposed simplified criteria (AVIO) to select optimal balloon size based on vessel area measurements. In several trials, the criteria for IVUS optimization relied on a comparison of the MLCSA of the stented segment with the distal reference area or with the mean reference vessel area.[39–41] This information is readily available with OCT, with the advantage of a reliable and fast automatic contour detection.

Expansion and sizing

OCT can quickly and accurately evaluate the result immediately after stent implantation, providing information on expansion, sizing, and apposition of the stent unmatched by angiography. A minimum stent area (MSA) lower than both the nominal stent and reference vessel areas defines underexpansion, whereas an MSA lower than the reference vessel area, but higher than the nominal stent area, defines undersizing. Although the concepts are clear, they are often difficult to translate into operational definitions for clinical application or research, so several variations can be found in the literature. OCT can measure MSA and lumen area of the reference vessel semi-automatically, thus giving a quick and accurate estimation of the expansion and sizing of the stent.

Apposition

Strut apposition is part of the criteria for optimal stent deployment. Imaging and pathological studies showed that incomplete stent apposition (ISA) is correlated with thrombus detection and late/very late stent thrombosis (L/VLST). ISA may delay neointimal healing of the stent[42–44] and incomplete endothelialization of the struts is a common morphological finding in fatal cases of L/VLST.[45,46] OCT is the most precise and sensitive technique to

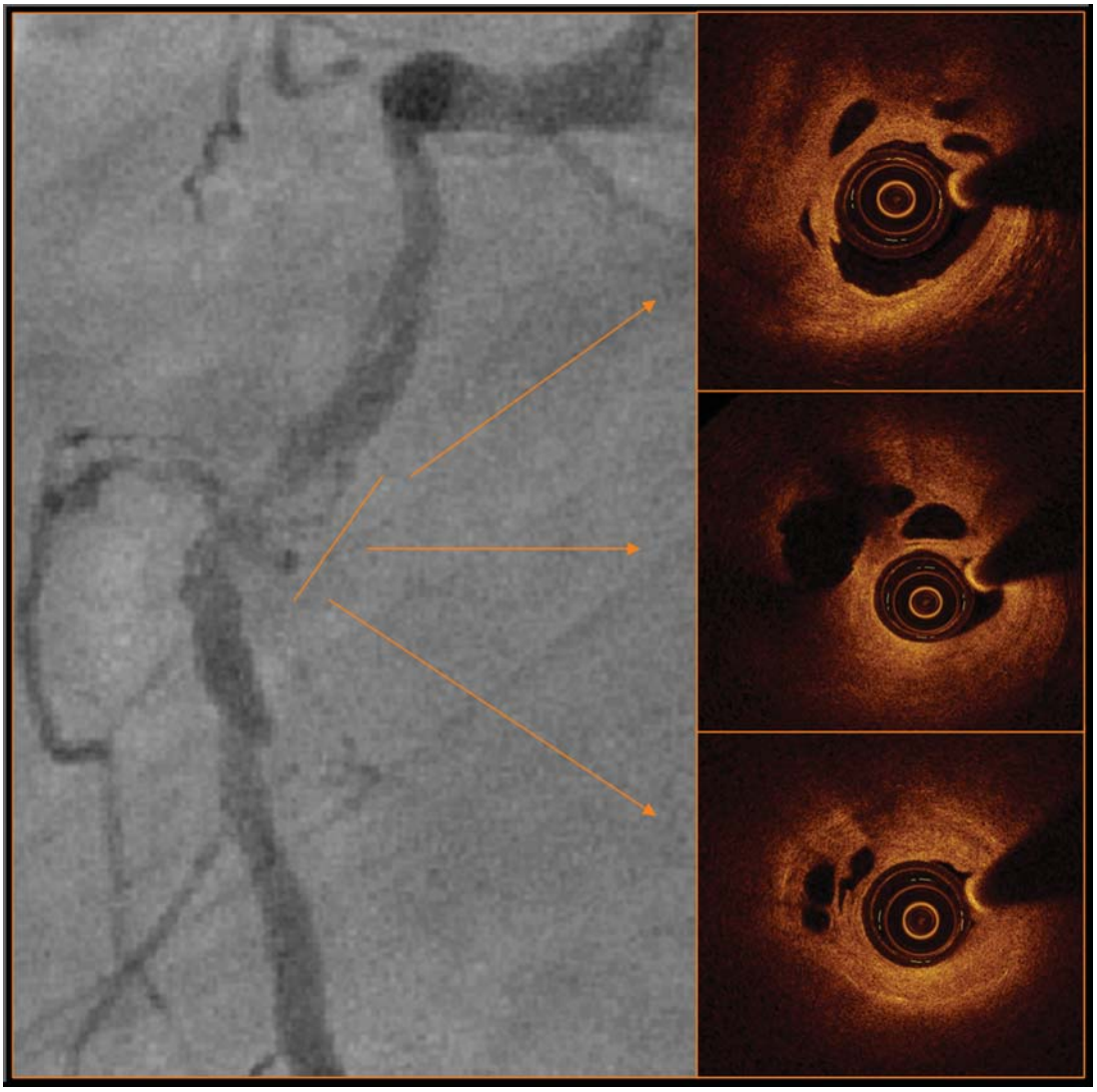

Figure 3 Coronary angiography of a 66-year-old patient with a heavily diseased right coronary artery and functional occlusion of the mid-segment after dilatation with a 2.0 mm balloon. Optical coherence tomography imaging reveals the presence of multiple additional microchannels measuring between 0.08 and 0.26 mm, explaining the easy crossing with a tapered hydrophilic wire (Fielder XT, Asahi, Japan).

evaluate apposition, being able to detect even subtle degrees of ISA that would remain unnoticed for other imaging techniques. Apposition is defined as the contact of the stent struts with the vessel wall. In metallic stents, the struts cast an optical shadow that hides the body of the strut and its abluminal side, thereby the contact between the strut and the vessel wall cannot be directly assessed by OCT, able to detect only the reflection produced at the adluminal face of the strut. Apposition is indirectly assessed by measuring the distance between the adluminal reflection of the strut and the vessel wall and comparing this distance with the strut thickness. ISA is then defined as a strut–vessel distance greater than the strut thickness (metal and polymer) with the addition of a correction factor[47] (*Figure 4*). *Table 3* shows the strut and polymer thickness for different types of modern drug-eluting stents (DESs). The use of a correction factor in the formula improves the specificity of the binary definition of apposition, following two different approaches. The first one consists of adding an empirical margin, usually ranging between 10–20 μm[42,44,48–55] and up to 30 μm[56] to take into account the axial resolution of the current OCT systems. The second approach corrects for strut 'blooming': the intense signal generated by the reflection of light against the metallic struts has an axial thickness itself. The true edge of the strut lies somewhere in the middle of the blooming. The so-called correction for blooming consists of measuring the blooming thickness in a random sample of study struts and then adding to the analysis of apposition a correction factor equal to half of the blooming thickness, ranging between 18[57,58] and 20 μm[59,60] in various studies. Although intense theoretical debate around these methodological issues is still ongoing, the practical impact of choosing one approach or the other is minimal, and maybe its importance should not be overemphasized.

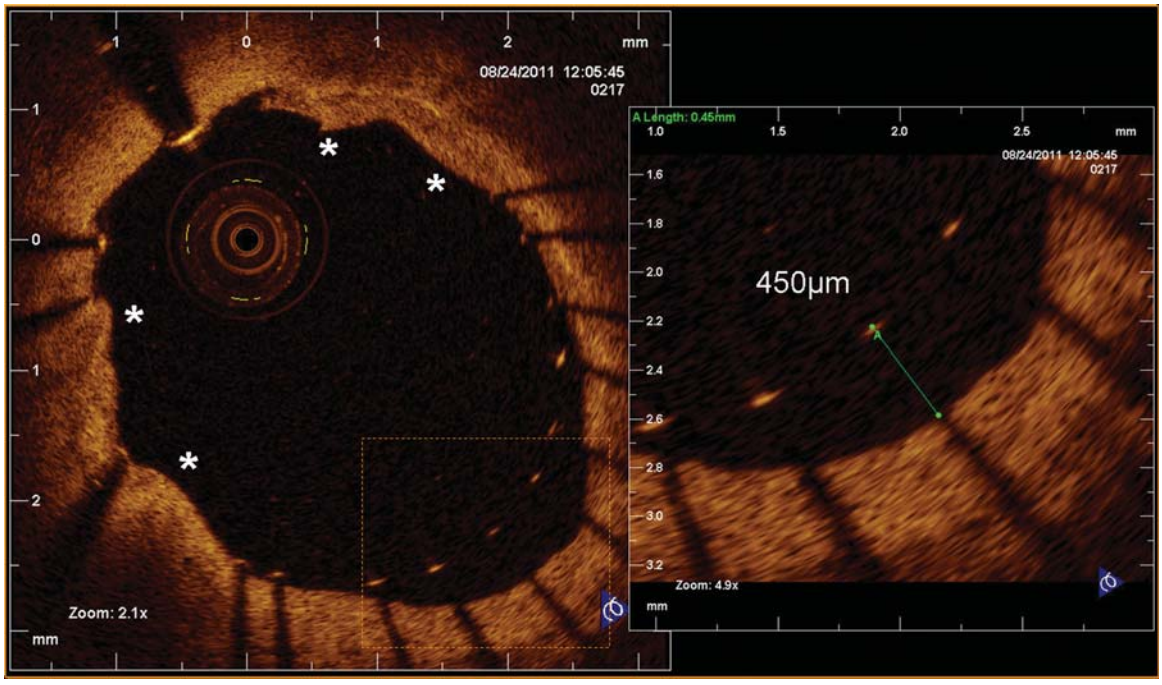

Figure 4 Assessment of intervention results immediately post-stent deployment. The cross-sections shows several points of mild tissue prolapse (asterisk) and incomplete stent apposition in the right lower quadrant. The measured strut–vessel distance was 450 µm (strut thickness = 81 µm).

Table 3 Strut and polymer thickness in different types of metallic stents

	Strut (µm)	Polymer (µm)	Total (µm)
Cypher Select	140	14	154
Taxus Element	132	16	148
Xience V	81	8	89
Resolute	91	6	97
Biomatrix	120	11	131
Vision	81	—	81

Bioresorbable intracoronary devices are made of polylactide, a crystallised translucent polymer that can be penetrated by optical radiation. In these devices, the abluminal side of the strut and its contact with or detachment from the vessel wall can be directly evaluated by OCT; therefore, the strut thickness is not required for the analysis of apposition.[61,62] A subclassification of well-apposed struts into embedded or protruding has been proposed,[47] depending on whether the strut–vessel distance is less or equal or greater than half of the corrected strut + polymer thickness, respectively. This discrimination might be of interest because of the flow disruption and potential increased thrombogenicity caused by protruding struts. This further subdivision, however, is of limited practical value for guidance of treatment because embedding is critically dependent on the composition of the subendothelial plaque components and not correctable, unlike apposition, with appropriate sizing and expansion at higher pressure.

In the struts jailing side branches, with no vessel wall behind, the evaluation of apposition is not possible. Initially, these struts were assimilated to ISA struts or excluded from the analysis.[57–60] However, it could make sense to consider them as an independent category of apposition, since recent evidence suggests that their biological meaning is substantially different from that of ISA struts.[44,63] The definition non-apposed side-branch struts (NASB) has been proposed for this category of struts.[44,51,53,64]

Vascular injury: dissections

OCT is very sensitive to detect subclinical dissections and microdissections, as well as other forms of vascular injury, like wire perforations, that usually remain unnoticed by angiography or IVUS (*Figure 5*).[65–67] Subclinical dissections and microdissections appear often at stent edges (edge dissections), but there is no evidence that they carry adverse prognostic implications. Likewise, it is uncertain whether the 'sealing' of subclinical dissections unveiled by OCT, for instance by overlapping additional stents, will translate into any clinical benefit for the patient.

Optical coherence tomography-guided coronary intervention

A small study on patients with ACS has proposed some criteria for guidance of percutaneous coronary intervention using FD-OCT. In intermediate (40–70% coronary stenosis) or hazy lesions, the decision to intervene was taken according to the following OCT

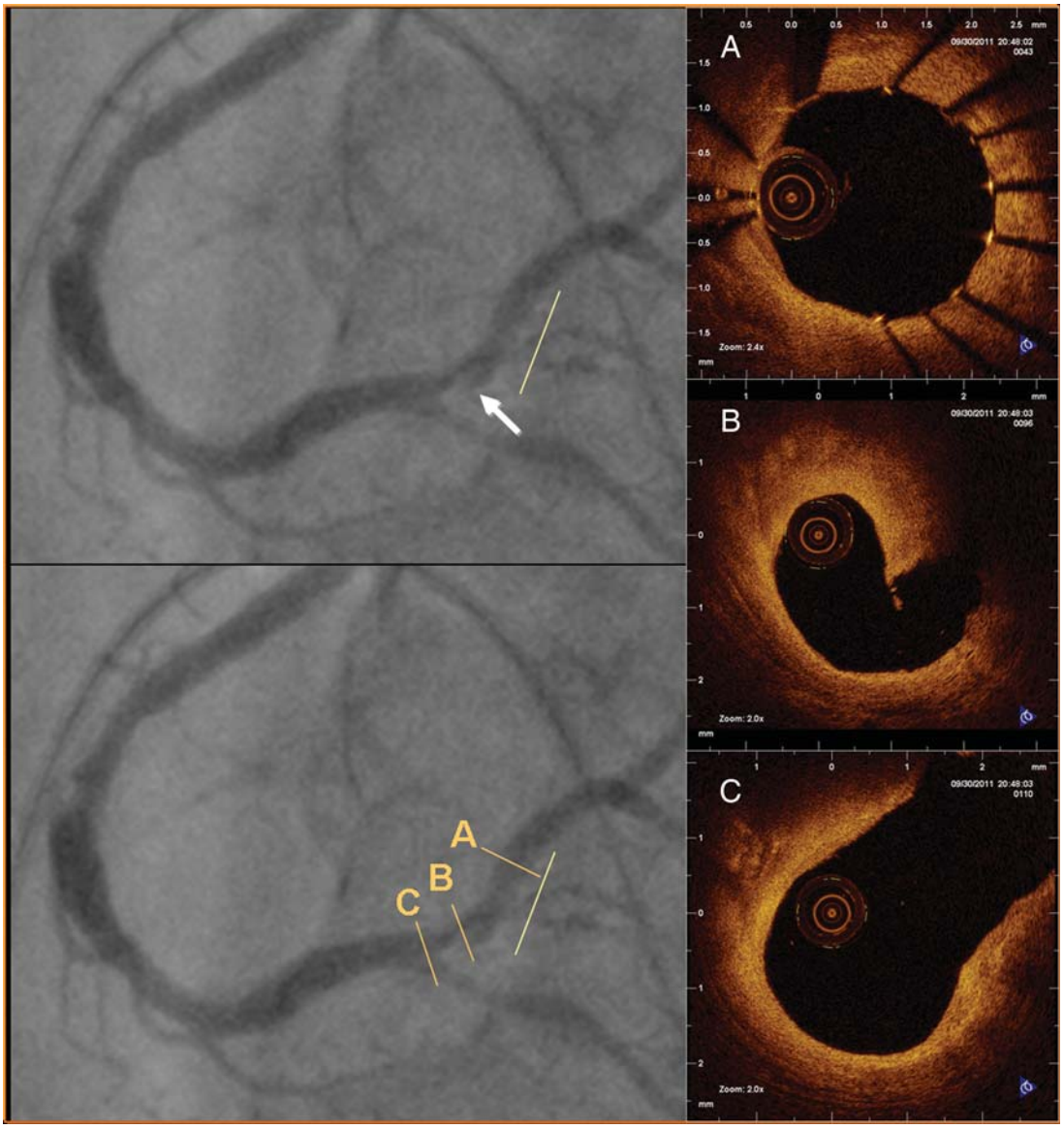

Figure 5 Proximal intraluminal filling defect (white arrow) in angiography after stent implantation (yellow line). Optical coherence tomography shows a thick proximal dissection in need of further stenting (*B*).

criteria: (i) MLCSA <3.5 mm^2 or (ii) presence of thrombus indicative of unstable plaque. The result after stent deployment was assessed by OCT and post-dilation/additional stent implantation was deemed necessary in case of: (i) underexpansion, (ii) significant ISA, (iii) edge dissection extending beyond 200 μm, or (iv) large plaque prolapse. This approach translated into high procedural success and good clinical results up to 5 months.[37] Another small study on patients with stable angina applied also OCT criteria for guidance of elective PCI[68] and reported separately results in a specific subgroup of bifurcational lesions.[69] Changes in the conventional strategy were prompted by serial OCT examinations in the majority of patients but, despite high-pressure post-dilatation and routine use of kissing-balloon dilatation, ISA remained high at the end of the procedure, particularly in calcified lesions and at the take-off of side branches (*Figure 6*).[69] Although these pilot studies prove the feasibility of OCT-guided coronary interventions and propose operative decision algorithms, we do not have to date any evidence that OCT-guided interventions translates into any advantage in terms of clinical outcomes when compared with conventional angiographic or IVUS guidance.

There is no evidence hitherto that the optimization of subtle degrees of ISA detected by OCT is associated with any clinical advantage. A recent study demonstrated that strut–vessel distances <270 μm are spontaneously corrected by the neointimal reaction in 100% of the cases (distances <400 μm, in 93% of the cases).[43]

Assessment at follow-up

IVUS has been classically the tool to quantify neointimal hyperplasia, but it lacks the axial resolution to evaluate the completeness of neointimal coverage in the DES era, when the average late lumen

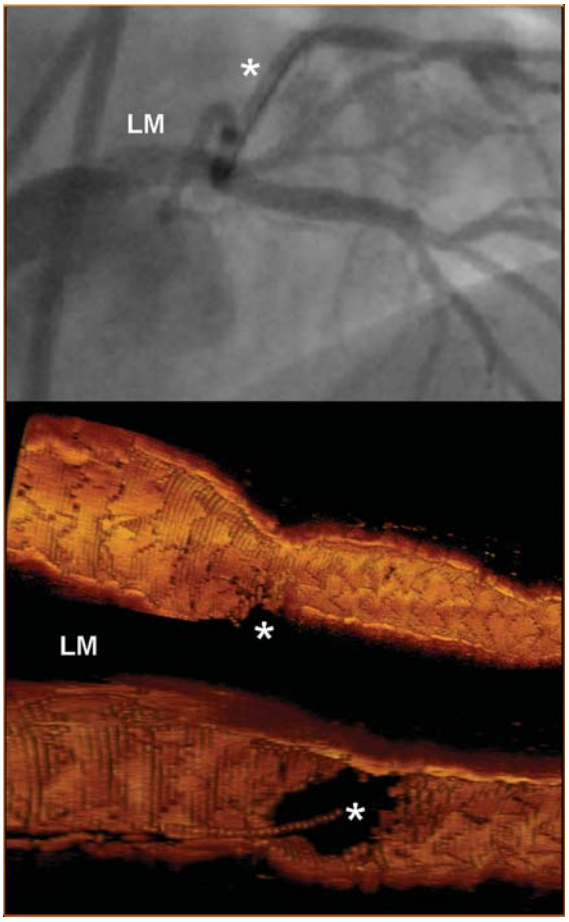

Figure 6 Left main stem (LM) stenting immediately post-implantation as seen by angiography (upper panel) and optical coherence tomography three-dimensional rendering (lower panel). Notice the guide wire placed in the circumflex (asterisk) to straighten the angle, and the detailed depiction of the circumflex opening after the kissing-balloon technique.

loss in modern second-generation stents is as low as 0.1–0.2 mm. OCT has 10-fold greater resolution than IVUS and has become an experimental tool for the evaluation of completeness of coverage *in vivo*. The interest for the completeness of coverage, and thereby for OCT, raised in parallel to the concerns about the risk of late and very late stent thrombosis associated with DESs.[70,71] Several pathology studies pointed to delayed neointimal healing as the underlying substrate in cases of fatal stent thrombosis.[45,46]

Quantitative analysis: volumetric analysis

Per cent neointimal volume obstruction is traditionally measured with IVUS to assess neointimal hyperplasia within stents and is used as an endpoint in trials comparing the performance of a DES vs. another DES or vs. a bare-metal stent (BMS).[57–60,64] OCT can provide the same information with greater accuracy.[18] Areas and volumetric parameters can also be used to characterize ISA. Corrected ISA volume expresses the absolute ISA volume as a percentage of the stent volume, similarly to the above explained

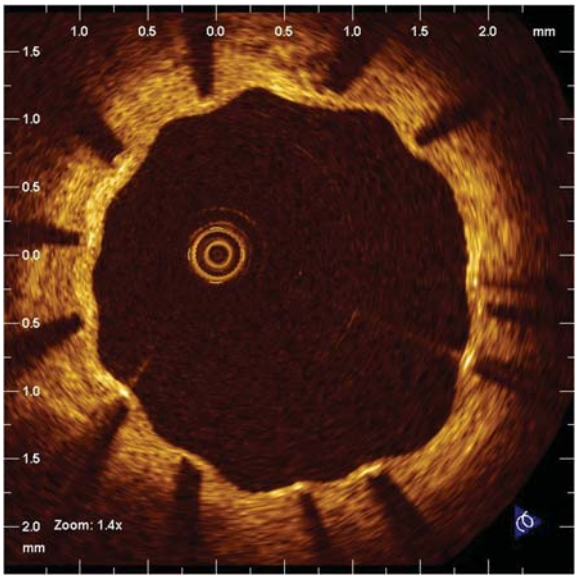

Figure 7 Covered struts in a drug-eluting stent 9 months after implantation. Notice the thin layer of tissue covering the struts and the typical corrugated appearance (crenellated pattern), found more often in drug-eluting stents.

per cent neointimal volume obstruction. However, recent studies suggest that absolute parameters, like absolute ISA volume or maximal ISA area, or maximal strut–vessel distance per strut, are better predictors of the neointimal reaction to malapposition.[43] Several sequential studies have reported that ISA areas and volumes tend to decrease spontaneously over time up to 24 months in different types of stents,[43,51,53] but one study addressing the long-term coverage of SES with serial OCT measurements found an increase in ISA between 24 and 48 months.[72]

Quantitative analysis: per-strut analysis

OCT also offers a detailed assessment strut by strut, which is far beyond the possibilities of any other intracoronary imaging technique.

The analysis of apposition at follow-up is performed following the same principles explained for the post-implantation study. The neointimal healing response after stenting tends to reduce the percentage of ISA struts over time up to 24 months in BMS and DES,[43,51,53] although one study has reported exactly the opposite in SES between 24 and 48 months.[72] A crenellated pattern at follow-up (i.e. containing many protruding struts) is associated with higher percentage of uncovered struts than smooth patterns of neointimal coverage.[43]

The assessment of neointimal coverage after stenting is the most important current research application of OCT. Coverage is evaluated as a binary outcome strut by strut (*Figure 7*) and has been used as a primary endpoint in most OCT trials and studies hitherto.[59,64,73,74] It is considered a surrogate for the completeness of neointimal healing, which is believed to be protective against stent thrombosis. Also the thickness of coverage can be also

Table 4 Summary of the percentage of uncovered struts and average thickness of coverage in the optical coherence tomographic studies published hitherto

Study	Design	Stent	FUP (months)	Uncovered struts (%)	NIT (μm)	Significance
Takano *et al.*[83]	Descriptive	SES	3	15.0	29 ± 41	NA
Matsumoto (2007)[48]	Descriptive	SES	6	9	52.5[a]	NA
Katoh *et al.*[50]	Descriptive, sequential	SES	6 12	10.4 5.7	112 ± 123 120 ± 130	NA
Yao *et al.*[52]	Descriptive	SES	6 12	10.5 7.9	42 ± 28 88 ± 32	NA
Ishigami *et al.*[56]	Descriptive	SES	<9 9–24 >25	14.8 11.7 4.1	53 ± 24 70 ± 41 99 ± 40	NA
Takano *et al.*[84]	Descriptive	SES	24	5.0	71 ± 93	NA
Takano *et al.*[72]	Descriptive, sequential	SES	24 48	3.2 0.9	77 ± 76 123 ± 103	NA
Davlouros in press[92]	Descriptive	PES	6	8.6	205 ± 160	NA
Kim (2009)[93]	Descriptive	ZES	3	0.1	137[a]	NA
Inoue *et al.*[55]	Descriptive	EES	8	1.7	80[a]	NA
Serruys 2009[61]	Descriptive, sequential	BVS 1.0	6 24	0 0	— —	NA
Serruys *et al.*[62]	Descriptive	BVS 1.1	6	3.2	—	NA
Chen *et al.*[78]	Comparative, observational	BMS BMS SES	7 45 9	0.3 0.3 7.0	200–500 220–610 40–120	S
Murakami (2009)[82]	Comparative, observational	SES PES	6	15.0 5.0	31 ± 39 118 ± 141	S
Kim *et al.*[81]	Comparative, observational	SES PES	9	12.5 4.9	86 ± 53 181 ± 105	S
Kim *et al.*[80]	Comparative, observational	ZES SES	9	0.3 12.3	251 ± 110 86 ± 53	S
Choi (2012)[79]	Comparative, observational	EES SES	9	4.4 10.5	115 ± 52 89 ± 58	S
Davlouros (in press)[94]	Comparative, observational	BES B-PES	6	0.41 0.21	59 ± 28 202 ± 98	S
Guagliumi *et al.*[58]	Comparative, randomized	PES BMS	13	5.7 1.1	170 ± 120 340 ± 170	S
Guagliumi *et al.*[60]	Comparative, randomized	ZES BMS	6	0.0 2.0	332[a] 186[a]	NS
Miyoshi *et al.*[54]	Comparative, randomized[b]	SES PES	6	12.7 6.6	50[a] 90[a]	S
Moore *et al.*[74]	Comparative, randomized	SES PF-SES	3	11.7 2.8	77 ± 26 191 ± 87	S
Guagliumi *et al.*[59]	Comparative, randomized	PES B-PES HD B-PES LD	6	5.3 7.0 4.6	200 ± 100 220 ± 150 240 ± 150	NS
Barlis *et al.*[73]	Comparative, randomized	BES SES	9	0.6 2.1	68[a] 57[a]	S (uncovered str) NS (NIT)
Gutiérrez-Chico (2011)[53]	Comparative, randomized, sequential	BES SES	9 24	2.8–1.5 5.7–1.8	58–86[a] 42–62[a]	NS (24 m)
Gutiérrez-Chico (2011)[64]	Comparative, randomized	R-ZES EES	13	7.4 5.8	116 ± 99 142 ± 113	NS
Gutiérrez-Chico *et al.*[51]	Comparative, randomized	DCB + BMS BMS + DCB	6	8.1 5.3	104[c] 132[c]	NS

NIT values are mean ± SD or minimum–maximum. Sample size (*n*) expressed as patients, lesions, stents, and struts (str). Significance expressed as significant (S), non-significant (NS), or non-applicable (NA). BES, biolimus-eluting stent; BMS, bare-metal stent; B-PES, paclitaxel-eluting stent with biodegradable polymer; BVS, bioresorbable vascular scaffold; DCB, drug-coated balloon; EES, everolimus-eluting stent; HD, high dose; LD, low dose; NIT, neointimal thickness; PES, paclitaxel-eluting stent; PF-SES, polymer-free sirolimus-eluting stent; R-ZES, zotarolimus-eluting stent with Biolynx polymer (Resolute™); SES, sirolimus-eluting stent; ZES, zotarolimus-eluting stent with phosphorylcholine polymer.

[a]Median.

[b]Within the same patient and the same coronary artery: randomization proximal vs. distal.

[c]Corrected mean (log transform).

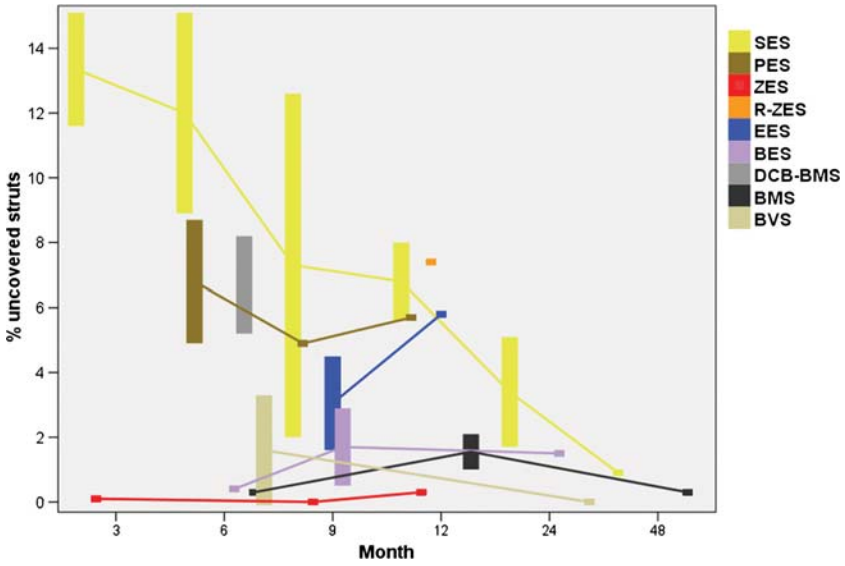

Figure 8 Reported coverage rates of the different stent types. Bars represent the maximum and minimum per cent of uncovered struts reported in peer-reviewed publications at each time point. In the case of one single study available, the value is represented by a square. Unweighted interpolation lines connect the values for each stent type, thus estimating the coverage rate of each device. BES, biolimus-eluting stent; BMS, bare-metal stent; BVS, bioresorbable vascular scaffold; DCB-BMS, combination of drug-coated balloon with bare-metal stent; EES, everolimus-eluting stent; PES, paclitaxel-eluting stent; R-ZES, zotarolimus-eluting stent with ByoLinx polymer (Resolute™); ZES, zotarolimus-eluting stent with phosphorylcholine polymer.

quantified strut by strut. Coverage assessed by OCT correlates with histological neointimal healing and endothelialization after stenting in animal models.[75,76] An important caveat is the inability of OCT to detect thin layers of neointima below its axial resolution (10–20 μm, limited sensitivity) and to discern between neointima and other material like fibrin or thrombus (limited specificity). The latter becomes an issue at very early phases after stenting, when the prevalence of struts covered by fibrin is high. Endothelial cells can be found on the metallic surface of the stent as early as Day 5 after implantation in a swine model, but these endothelial cells restore the endothelial continuity very seldom, and areas devoid of endothelium appear covered by granulation tissue or fibrin.[77] Thus, DESs are completely covered with fibrin (not with neointima) 1–3 days after implantation, but the low discriminative power of OCT results in false coverage rates of 45–76%.[76] The analysis of optical density might overcome this limitation in the future and discern between neointima and fibrin.[76] Since the greatest interest is to assess intimal coverage at late follow-up, months or years after stent implantation, when the prevalence of fibrin-covered struts is low, the practical impact of this limitation is minimal.[75]

Table 4 summarizes all the OCT studies reporting coverage of intracoronary devices published hitherto, with the corresponding percentage of uncovered struts and average thickness of coverage for each stent. SES is the most extensively studied stent, with data assessing coverage between 3 and 48 months.[42,48–50,52–54,56,57,63,72–74,78–85] More recently, large OCT trials have focused on PES and second-generation stents.[58,64] The absolute measurements are difficult to compare because studies addressed different populations, different clinical settings, and used different methodology of analysis. Moreover, only a few studies are truly sequential.[42,43,50,51,53,61,72] However, irrespective of these limitations, these studies provide a raw estimation of the coverage rates at each time point for the different stents examined (*Figure 8*). Coverage of DESs with durable polymers is delayed with respect to that of BMS, with the exception of ZES with phosphorylcholine polymer. DESs with biodegradable polymers and bioresorbable vascular scaffolds show coverage rates in the range of those reported for BMS. Interestingly, the coverage of BMS shifts to the range of PES, when it is implanted in combination with paclitaxel-coated balloon, what serves as an additional proof of concept of the effectiveness of this drug-delivery technology.[51]

The analysis of strut coverage by OCT has contributed to a better understanding of the neointimal healing response in specific scenarios. Coverage of ISA and NASB struts is delayed compared with well-apposed struts.[42,44] Coverage of NASB struts in DESs is delayed in comparison to NASB struts in BMS.[63] Finally, coverage of ISA struts is delayed with respect to NASB struts in DESs.[44] These findings suggest that the detachment of struts from the vessel wall poses higher risk of delayed coverage than a correct apposition in DES, but this risk is higher if the detachment is due to malapposition (ISA) than to the presence of a side branch (NASB). A possible explanation for these differences is the fact that ISA is caused by the presence of more severely diseased vessel segments resulting in distorted stent geometry and irregular drug release, impairing healing. This phenomenon is not present in NASB struts, which are also protected by the continuous flow through the side-branch origin.[44] Similarly, the coverage of overlapping segments is delayed compared with non-overlapping segments in DES[86] and with overlapping segments in BMS.[57]

Table 5 Discrepancy between the rates of definite and probable stent thrombosis in clinical trials comparing different types of stents and the coverage measured in the corresponding optical coherence tomographic substudies of these trials

Clinical trial	LEADERS 9m[95]	HORIZONS-AMI[96]	RESOLUTE-AC[97]
Patients (*n*)	1707	3006	2292
Stents	BES vs. SES	PES vs. BMS	R-ZES vs. EES
Differences in definite + probable ST?	NO 2.6 vs. 2.2% $P = 0.66$	NO 3.2 vs. 3.4% $P = 0.77$	YES 1.6 vs. 0.7% $P = 0.05$
OCT substudy[73,58,64]			
Patients (*n*)	56	118	58
Differences in coverage?	YES 0.6 vs.2.1% $P = 0.04$	YES 5.7 vs. 1.1% $P < 0.0001$	NO 7.4 vs. 5.8% $P = 0.378$

BES, biolimus-eluting stent; BMS, bare-metal stent; EES, everolimus-eluting stent; PES, paclitaxel-eluting stent; R-ZES, zotarolimus-eluting stent with Biolynx polymer (Resolute™); SES, sirolimus-eluting stent; ST, stent thrombosis.

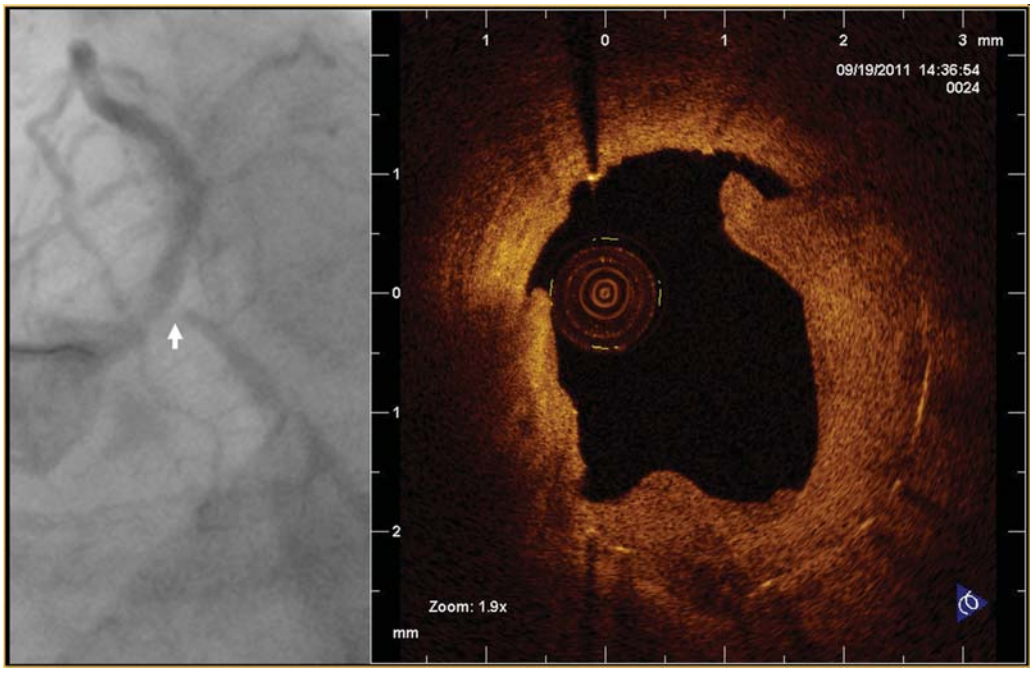

Figure 9 Restenosis of a bare-metal stent implanted at the ostium of the left circumflex (white arrow) in the 5th month post-implantation. After plain old balloon predilatation, optical coherence tomography shows optically homogeneous neointima with uneven disruption and persistence of a large amount of restenotic tissue.

While there starts to be consensus about accepting the coverage assessed by OCT as a valid surrogate for neointimal coverage, the association of coverage with thrombosis propensity is more controversial due to the lack of sufficiently large longitudinal studies. The largest OCT studies only included hundreds of patients, so they were grossly underpowered to detect a phenomenon with so low incidence as stent thrombosis. An interesting source to explore this association was the OCT substudies conducted within large clinical trials. Paradoxically, OCT substudies in those trials without significant differences in thrombosis found differences in coverage,[58,73] whereas the OCT substudies of those trials with significant differences in thrombosis did not find any difference in coverage rates[64] (*Table 5*). Methodological issues or the long-term evolution of coverage[53] might be the key to understand this apparent paradox. OCT has opened a new perspective over the neointimal healing process, and the lessons learned from it must be still properly understood.

Qualitative assessment

Besides the quantification of NIH and stent coverage, OCT can make a qualitative evaluation of the covering tissue.[87,88] Several patterns have been described, according to the optical homogeneity or to the presence of neovascularization,[87] but their meaning is still uncertain. Heterogeneous patterns have been initially described in the Taxus™ (Boston Scientific, Natick, MA, USA) stent,[89] but later on in many other stents.[43,55,64] Optically, heterogeneous tissue has been also associated with focal and edge restenosis,[87] with the presence of fibrinoid or proteoglycans,[90,91] and with the resolution of acute ISA (layered patterns).[43] It has been hypothesized that it might also correspond to endothelialisation over thrombotic material, with no demonstration so far.

Early in-stent restenosis (<6 months) is optically homogeneous, especially in BMS (*Figure 9*), while very late restenosis (>5 years) presents images of lipid pools and calcification, suggesting a prominent role of atherosclerosis progression as a pathogenic mechanism.[88]

Final conclusions

While the introduction of intracoronary OCT has significantly advanced our understanding of plaque morphology and mechanisms underlying ACS, considerable further work is required to establish robust criteria offering advantages over established clinical parameters and biomarkers for risk stratification. With the development of frequency-domain OCT, the technique has become applicable for guidance of coronary interventions with a greater potential for immediate quantification of stent apposition and expansion compared with IVUS. Follow-up studies indicate that malapposed struts are prone to slower and incomplete coverage and detect differences among various stent platforms.

An enormous amount of work is still required to validate the clinical relevance of the various OCT applications. At this stage, it is fair to say that the perception that OCT is only a playtool generating 'pretty pictures' is ungenerous towards a technique which has the potential to become a generally accepted auxiliary technique in the research and practice of interventional cardiology.

Conflict of interest: none declared.

Funding

The Open Access of this review has been sponsored by a grant from Saint Jude Medical.

References

1. Spears JR, Sandor T, Als AV, Malagold M, Markis JE, Grossman W *et al.* Computerized image analysis for quantitative measurement of vessel diameter from cineangiograms. *Circulation* 1983;**68**:453–61.
2. Reiber JH, Serruys PW, Kooijman CJ, Wijns W, Slager CJ, Gerbrands JJ *et al.* Assessment of short-, medium-, and long-term variations in arterial dimensions from computer-assisted quantitation of coronary cineangiograms. *Circulation* 1985;**71**: 280–8.
3. Abizaid A, Mintz GS, Pichard AD, Kent KM, Satler LF, Walsh CL *et al.* Clinical, intravascular ultrasound, and quantitative angiographic determinants of the coronary flow reserve before and after percutaneous transluminal coronary angioplasty. *Am J Cardiol* 1998;**82**:423–8.
4. Briguori C, Anzuini A, Airoldi F, Gimelli G, Nishida T, Adamian M *et al.* Intravascular ultrasound criteria for the assessment of the functional significance of intermediate coronary artery stenoses and comparison with fractional flow reserve. *Am J Cardiol* 2001;**87**:136–41.
5. Nishioka T, Amanullah AM, Luo H, Berglund H, Kim CJ, Nagai T *et al.* Clinical validation of intravascular ultrasound imaging for assessment of coronary stenosis severity: comparison with stress myocardial perfusion imaging. *J Am Coll Cardiol* 1999;**33**:1870–8.
6. Nam CW, Yoon HJ, Cho YK, Park HS, Kim H, Hur SH *et al.* Outcomes of percutaneous coronary intervention in intermediate coronary artery disease: fractional flow reserve-guided versus intravascular ultrasound-guided. *JACC Cardiovasc Interv* 2010;**3**:812–7.
7. Ahn JM, Kang SJ, Mintz GS, Oh JH, Kim WJ, Lee JY *et al.* Validation of minimal luminal area measured by intravascular ultrasound for assessment of functionally significant coronary stenosis: comparison with myocardial perfusion imaging. *JACC Cardiovasc Interv* 2011;**4**:665–71.
8. Ben-Dor I, Torguson R, Gaglia MA Jr, Gonzalez MA, Maluenda G, Bui AB *et al.* Correlation between fractional flow reserve and intravascular ultrasound lumen area in intermediate coronary artery stenosis. *EuroIntervention* 2011;**7**:225–33.
9. Bech GJW, De Bruyne B, Pijls NHJ, de Muinck ED, Hoorntje JCA, Escaned J *et al.* Fractional flow reserve to determine the appropriateness of angioplasty in moderate coronary stenosis: a randomized trial. *Circulation* 2001;**103**:2928–34.
10. Tonino PAL, De Bruyne B, Pijls NHJ, Siebert U, Ikeno F, Veer M *et al.* Fractional flow reserve versus angiography for guiding percutaneous coronary intervention. *N Engl J Med* 2009;**360**:213–24.
11. Gonzalo N, Serruys PW, Garcia-Garcia HM, van Soest G, Okamura T, Ligthart J *et al.* Quantitative ex vivo and *in vivo* comparison of lumen dimensions measured by optical coherence tomography and intravascular ultrasound in human coronary arteries. *Rev Esp Cardiol* 2009;**62**:615–24.
12. Kawase Y, Hoshino K, Yoneyama R, McGregor J, Hajjar RJ, Jang IK *et al.* *In vivo* volumetric analysis of coronary stent using optical coherence tomography with a novel balloon occlusion-flushing catheter: a comparison with intravascular ultrasound. *Ultrasound Med Biol* 2005;**31**:1343–9.
13. Gonzalo N, Garcia-Garcia HM, Serruys PW, Commissaris KH, Bezerra H, Gobbens P *et al.* Reproducibility of quantitative optical coherence tomography for stent analysis. *EuroIntervention* 2009;**5**:224–32.
14. Gutierrez-Chico JL, Serruys PW, Girasis C, Garg S, Onuma Y, Brugaletta S *et al.* Quantitative multi-modality imaging analysis of a fully bioresorbable stent: a head-to-head comparison between QCA, IVUS and OCT. *Int J Cardiovasc Imaging* 2011 (Epub ahead of print).
15. Fox KA, Dabbous OH, Goldberg RJ, Pieper KS, Eagle KA, Van de WF *et al.* Prediction of risk of death and myocardial infarction in the six months after presentation with acute coronary syndrome: prospective multinational observational study (GRACE). *Br Med J* 2006;**333**:1091.
16. Vancraeynest D, Pasquet A, Roelants V, Gerber BL, Vanoverschelde JL. Imaging the vulnerable plaque. *J Am Coll Cardiol* 2011;**57**:1961–79.
17. Stone GW, Maehara A, Lansky AJ, de BB, Cristea E, Mintz GS *et al.* A prospective natural-history study of coronary atherosclerosis. *N Engl J Med* 2011;**364**:226–35.
18. Kume T, Akasaka T, Kawamoto T, Watanabe N, Toyota E, Neishi Y *et al.* Assessment of coronary intima–media thickness by optical coherence tomography: comparison with intravascular ultrasound. *Circ J* 2005;**69**:903–7.
19. Yamaguchi T, Terashima M, Akasaka T, Hayashi T, Mizuno K, Muramatsu T *et al.* Safety and feasibility of an intravascular optical coherence tomography image wire system in the clinical setting. *Am J Cardiol* 2008;**101**:562–7.
20. Yabushita H, Bouma BE, Houser SL, Aretz HT, Jang IK, Schlendorf KH *et al.* Characterization of human atherosclerosis by optical coherence tomography. *Circulation* 2002;**106**:1640–5.
21. Kume T, Akasaka T, Kawamoto T, Watanabe N, Toyota E, Neishi Y *et al.* Assessment of coronary arterial plaque by optical coherence tomography. *Am J Cardiol* 2006;**97**:1172–5.
22. Kume T, Akasaka T, Kawamoto T, Ogasawara Y, Watanabe N, Toyota E *et al.* Assessment of coronary arterial thrombus by optical coherence tomography. *Am J Cardiol* 2006;**97**:1713–7.
23. Kume T, Akasaka T, Kawamoto T, Okura H, Watanabe N, Toyota E *et al.* Measurement of the thickness of the fibrous cap by optical coherence tomography. *Am Heart J* 2006;**152**:755.e1–4.
24. Jang IK, Tearney GJ, MacNeill B, Takano M, Moselewski F, Iftima N *et al.* *In vivo* characterization of coronary atherosclerotic plaque by use of optical coherence tomography. *Circulation* 2005;**111**:1551–5.
25. Kubo T, Imanishi T, Takarada S, Kuroi A, Ueno S, Yamano T *et al.* Assessment of culprit lesion morphology in acute myocardial infarction: ability of optical coherence tomography compared with intravascular ultrasound and coronary angioscopy. *J Am Coll Cardiol* 2007;**50**:933–9.
26. Naghavi M, Libby P, Falk E, Casscells SW, Litovsky S, Rumberger J *et al.* From vulnerable plaque to vulnerable patient: a call for new definitions and risk assessment strategies: Part I. *Circulation* 2003;**108**:1664–72.
27. Virmani R, Kolodgie FD, Burke AP, Finn AV, Gold HK, Tulenko TN *et al.* Atherosclerotic plaque progression and vulnerability to rupture: angiogenesis as a source of intraplaque hemorrhage. *Arterioscler Thromb Vasc Biol* 2005;**25**:2054–61.

28. Fujii K, Masutani M, Okumura T, Kawasaki D, Akagami T, Ezumi A *et al.* Frequency and predictor of coronary thin-cap fibroatheroma in patients with acute myocardial infarction and stable angina pectoris a 3-vessel optical coherence tomography study. *J Am Coll Cardiol* 2008;**52**:787–8.
29. Sawada T, Shite J, Garcia-Garcia HM, Shinke T, Watanabe S, Otake H *et al.* Feasibility of combined use of intravascular ultrasound radiofrequency data analysis and optical coherence tomography for detecting thin-cap fibroatheroma. *Eur Heart J* 2008;**29**:1136–46.
30. Tanaka A, Imanishi T, Kitabata H, Kubo T, Takarada S, Tanimoto T *et al.* Lipid-rich plaque and myocardial perfusion after successful stenting in patients with non-ST-segment elevation acute coronary syndrome: an optical coherence tomography study. *Eur Heart J* 2009;**30**:1348–55.
31. Kubo T, Imanishi T, Kashiwagi M, Ikejima H, Tsujioka H, Kuroi A *et al.* Multiple coronary lesion instability in patients with acute myocardial infarction as determined by optical coherence tomography. *Am J Cardiol* 2010;**105**:318–22.
32. Toutouzas K, Tsiamis E, Karanasos A, Drakopoulou M, Synetos A, Tsioufis C *et al.* Morphological characteristics of culprit atheromatic plaque are associated with coronary flow after thrombolytic therapy: new implications of optical coherence tomography from a multicenter study. *JACC Cardiovasc Interv* 2010;**3**:507–14.
33. Ino Y, Kubo T, Tanaka A, Kuroi A, Tsujioka H, Ikejima H *et al.* Difference of culprit lesion morphologies between ST-segment elevation myocardial infarction and non-ST-segment elevation acute coronary syndrome: an optical coherence tomography study. *JACC Cardiovasc Interv* 2011;**4**:76–82.
34. Tanaka A, Imanishi T, Kitabata H, Kubo T, Takarada S, Tanimoto T *et al.* Morphology of exertion-triggered plaque rupture in patients with acute coronary syndrome: an optical coherence tomography study. *Circulation* 2008;**118**:2368–73.
35. Fujii K, Kawasaki D, Masutani M, Okumura T, Akagami T, Sakoda T *et al.* OCT assessment of thin-cap fibroatheroma distribution in native coronary arteries. *JACC Cardiovasc Imaging* 2010;**3**:168–75.
36. Cheruvu PK, Finn AV, Gardner C, Caplan J, Goldstein J, Stone GW *et al.* Frequency and distribution of thin-cap fibroatheroma and ruptured plaques in human coronary arteries: a pathologic study. *J Am Coll Cardiol* 2007;**50**:940–9.
37. Imola F, Mallus MT, Ramazzotti V, Manzoli A, Pappalardo A, Di GA *et al.* Safety and feasibility of frequency domain optical coherence tomography to guide decision making in percutaneous coronary intervention. *EuroIntervention* 2010;**6**:575–81.
38. Gerber RT, Latib A, Ielasi A, Cosgrave J, Qasim A, Airoldi F *et al.* Defining a new standard for IVUS optimized drug eluting stent implantation: the PRAVIO study. *Catheter Cardiovasc Interv* 2009;**74**:348–56.
39. de Jaegere P, Mudra H, Figulla H, Almagor Y, Doucet S, Penn I *et al.* Intravascular ultrasound-guided optimized stent deployment. Immediate and 6 months clinical and angiographic results from the Multicenter Ultrasound Stenting in Coronaries Study (MUSIC Study). *Eur Heart J* 1998;**19**:1214–23.
40. Albiero R, Rau T, Schluter M, Di MC, Reimers B, Mathey DG *et al.* Comparison of immediate and intermediate-term results of intravascular ultrasound versus angiography-guided Palmaz–Schatz stent implantation in matched lesions. *Circulation* 1997;**96**:2997–3005.
41. Fitzgerald PJ, Oshima A, Hayase M, Metz JA, Bailey SR, Baim DS *et al.* Final results of the Can Routine Ultrasound Influence Stent Expansion (CRUISE) study. *Circulation* 2000;**102**:523–30.
42. Ozaki Y, Okumura M, Ismail TF, Naruse H, Hattori K, Kan S *et al.* The fate of incomplete stent apposition with drug-eluting stents: an optical coherence tomography-based natural history study. *Eur Heart J* 2010;**31**:1470–6.
43. Gutiérrez-Chico J, Wykrzykowska JJ, Nüesch E, van Geuns RJ, Koch K, Koolen JJ *et al.* Vascular tissue reaction to acute malapposition in human coronary arteries: sequential assessment with optical coherence tomography. *Circ Cardiovasc Interv* 2012 (in press).
44. Gutiérrez-Chico JL, Regar E, Nüesch E, Okamura T, Wykrzykowska J, di Mario C *et al.* Delayed coverage in malapposed and side-branch struts with respect to well-apposed struts in drug-eluting stents. *Circulation* 2011;**124**:612–23.
45. Finn AV, Joner M, Nakazawa G, Kolodgie F, Newell J, John MC *et al.* Pathological correlates of late drug-eluting stent thrombosis: strut coverage as a marker of endothelialization. *Circulation* 2007;**115**:2435–41.
46. Virmani R, Guagliumi G, Farb A, Musumeci G, Grieco N, Motta T *et al.* Localized hypersensitivity and late coronary thrombosis secondary to a sirolimus-eluting stent: should we be cautious? *Circulation* 2004;**109**:701–5.
47. Tanigawa J, Barlis P, di Mario C. Intravascular optical coherence tomography: optimisation of image acquisition and quantitative assessment of stent strut apposition. *EuroIntervention* 2007;**3**:128–36.
48. Matsumoto D, Shite J, Shinke T, Otake H, Tanino Y, Ogasawara D *et al.* Neointimal coverage of sirolimus-eluting stents at 6-month follow-up: evaluated by optical coherence tomography. *Eur Heart J* 2007;**28**:961–7.
49. Kubo T, Imanishi T, Kitabata H, Kuroi A, Ueno S, Yamano T *et al.* Comparison of vascular response after sirolimus-eluting stent implantation between patients with unstable and stable angina pectoris: a serial optical coherence tomography study. *JACC Cardiovasc Imaging* 2008;**1**:475–84.
50. Katoh H, Shite J, Shinke T, Matsumoto D, Tanino Y, Ogasawara D *et al.* Delayed neointimalization on sirolimus-eluting stents: 6-month and 12-month follow up by optical coherence tomography. *Circ J* 2009;**73**:1033–7.
51. Gutiérrez-Chico J, van Geuns RJ, Koch K, Koolen J, Duckers HJ, Regar E *et al.* Paclitaxel-coated balloon in combination with bare metal stent for treatment of de novo coronary lesions: an optical coherence tomography first-in-human randomized trial balloon-first vs. stent first. *EuroIntervention* 2011;**7**:711–22.
52. Yao ZH, Matsubara T, Inada T, Suzuki Y, Suzuki T. Neointimal coverage of sirolimus-eluting stents 6 months and 12 months after implantation: evaluation by optical coherence tomography. *Chin Med J (Engl)* 2008;**121**:503–7.
53. Gutiérrez-Chico J, Jüni P, García-García HM, Regar E, Nüesch E, Borgia F *et al.* Long term tissue coverage of a biodegradable polylactide polymer-coated biolimus-eluting stent: comparative sequential assessment with optical coherence tomography until complete resorption of the polymer. *Am Heart J* 2011;**162**:922–31.
54. Miyoshi N, Shite J, Shinke T, Otake H, Tanino Y, Ogasawara D *et al.* Comparison by optical coherence tomography of paclitaxel-eluting stents with sirolimus-eluting stents implanted in one coronary artery in one procedure. 6-month follow-up. *Circ J* 2010;**74**:903–8.
55. Inoue T, Shite J, Yoon J, Shinke T, Otake H, Sawada T *et al.* Optical coherence evaluation for everolimus-eluting stents at 8 months after implantation (Cooperative Study with Korea). *Heart* 2010;**97**:1379–84.
56. Ishigami K, Uemura S, Morikawa Y, Soeda T, Okayama S, Nishida T *et al.* Long-term follow-up of neointimal coverage of sirolimus-eluting stents—evaluation with optical coherence tomography. *Circ J* 2009;**73**:2300–7.
57. Guagliumi G, Musumeci G, Sirbu V, Bezerra HG, Suzuki N, Fiocca L *et al.* Optical coherence tomography assessment of *in vivo* vascular response after implantation of overlapping bare-metal and drug-eluting stents. *JACC Cardiovasc Interv* 2010;**3**:531–9.
58. Guagliumi G, Costa MA, Sirbu V, Musumeci G, Bezerra HG, Suzuki N *et al.* Strut coverage and late malapposition with paclitaxel-eluting stents compared with bare metal stents in acute myocardial infarction: optical coherence tomography substudy of the Harmonizing Outcomes With Revascularization and Stents in Acute Myocardial Infarction (HORIZONS-AMI) trial. *Circulation* 2011;**123**:274–81.
59. Guagliumi G, Sirbu V, Musumeci G, Bezerra HG, Aprile A, Kyono H *et al.* Strut coverage and vessel wall response to a new-generation paclitaxel-eluting stent with an ultrathin biodegradable abluminal polymer: Optical Coherence Tomography Drug-Eluting Stent Investigation (OCTDESI). *Circ Cardiovasc Interv* 2010;**3**:367–75.
60. Guagliumi G, Sirbu V, Bezerra H, Biondi-Zoccai G, Fiocca L, Musumeci G *et al.* Strut coverage and vessel wall response to zotarolimus-eluting and bare-metal stents implanted in patients with ST-segment elevation myocardial infarction: the OCTAMI (Optical Coherence Tomography in Acute Myocardial Infarction) Study. *JACC Cardiovasc Interv* 2010;**3**:680–7.
61. Serruys PW, Ormiston JA, Onuma Y, Regar E, Gonzalo N, Garcia-Garcia HM *et al.* A bioabsorbable everolimus-eluting coronary stent system (ABSORB): 2-year outcomes and results from multiple imaging methods. *Lancet* 2009;**373**:897–910.
62. Serruys PW, Onuma Y, Ormiston JA, De Bruyne B, Regar E, Dudek D *et al.* Evaluation of the second generation of a bioresorbable everolimus drug-eluting vascular scaffold for treatment of de novo coronary artery stenosis: 6-month clinical and imaging outcomes. *Circulation* 2010;**122**:2301–12.
63. Liu Y, Imanishi T, Kubo T, Tanaka A, Kitabata H, Tanimoto T *et al.* Assessment by optical coherence tomography of stent struts across side branch. Comparison of bare-metal stents and drug-elution stents. *Circ J* 2010;**75**:106–12.
64. Gutierrez-Chico JL, van Geuns RJ, Regar E, van der Giessen WJ, Kelbaek H, Saunamaki K *et al.* Tissue coverage of a hydrophilic polymer-coated zotarolimus-eluting stent vs. a fluoropolymer-coated everolimus-eluting stent at 13-month follow-up: an optical coherence tomography substudy from the RESOLUTE All Comers trial. *Eur Heart J* 2011;**32**:2454–63.
65. Gonzalo N, Serruys PW, Okamura T, Shen ZJ, Garcia-Garcia HM, Onuma Y *et al.* Relation between plaque type and dissections at the edges after stent implantation: An optical coherence tomography study. *Int J Cardiol* 2011;**150**:151–5.
66. Gonzalo N, Serruys PW, Okamura T, Shen ZJ, Onuma Y, Garcia-Garcia HM *et al.* Optical coherence tomography assessment of the acute effects of stent implantation on the vessel wall: a systematic quantitative approach. *Heart* 2009;**95**:1913–9.
67. Shin ES, Garcia-Garcia HM, Okamura T, Wykrzykowska JJ, Gonzalo N, Shen ZJ *et al.* Comparison of acute vessel wall injury after self-expanding stent and conventional balloon-expandable stent implantation: a study with optical coherence tomography. *J Invasive Cardiol* 2010;**22**:435–9.

68. Viceconte N, Chan P, Ghilencea L, Lindsay A, Foin N, di Mario C. Frequency domain optical coherence tomography for guidance of coronary stenting. *Int J Cardiol* 2012 (Epub ahead of print).
69. Viceconte N, Tyczynski P, Ferrante G, Foin N, Chan P, Alegría-Barrero E *et al.* Immediate results of bifurcational stenting assessed with optical coherence tomography. *Cathet Cardiovasc Intervent* 2012 (in press).
70. Iakovou I, Schmidt T, Bonizzoni E, Ge L, Sangiorgi GM, Stankovic G *et al.* Incidence, predictors, and outcome of thrombosis after successful implantation of drug-eluting stents. *J Am Med Assoc* 2005;**293**:2126–30.
71. Lagerqvist B, James SK, Stenestrand U, Lindback J, Nilsson T, Wallentin L, the SCAAR Study Group. Long-term outcomes with drug-eluting stents versus bare-metal stents in Sweden. *N Engl J Med* 2007;**356**:1009–19.
72. Takano M, Yamamoto M, Mizuno M, Murakami D, Inami T, Kimata N *et al.* Late vascular responses from 2 to 4 years after implantation of sirolimus-eluting stents: serial observations by intracoronary optical coherence tomography. *Circ Cardiovasc Interv* 2010;**3**:476–83.
73. Barlis P, Regar E, Serruys PW, Dimopoulos K, van der Giessen WJ, van Geuns RJ *et al.* An optical coherence tomography study of a biodegradable vs. durable polymer-coated limus-eluting stent: a LEADERS trial sub-study. *Eur Heart J* 2010;**31**:165–76.
74. Moore P, Barlis P, Spiro J, Ghimire G, Roughton M, Di MC *et al.* A randomized optical coherence tomography study of coronary stent strut coverage and luminal protrusion with rapamycin-eluting stents. *JACC Cardiovasc Interv* 2009;**2**: 437–44.
75. Murata A, Wallace-Bradley D, Tellez A, Alviar C, Aboodi M, Sheehy A *et al.* Accuracy of optical coherence tomography in the evaluation of neointimal coverage after stent implantation. *JACC Cardiovasc Imaging* 2010;**3**:76–84.
76. Templin C, Meyer M, Muller MF, Djonov V, Hlushchuk R, Dimova I *et al.* Coronary optical frequency domain imaging (OFDI) for *in vivo* evaluation of stent healing: comparison with light and electron microscopy. *Eur Heart J* 2010;**31**:1792–801.
77. van Beusekom HM, Sorop O, van den HM, Onuma Y, Duncker DJ, Danser AH *et al.* Endothelial function rather than endothelial restoration is altered in paclitaxel- as compared to bare metal-, sirolimus and tacrolimus-eluting stents. *EuroIntervention* 2010;**6**:117–25.
78. Chen BX, Ma FY, Luo W, Ruan JH, Xie WL, Zhao XZ *et al.* Neointimal coverage of bare-metal and sirolimus-eluting stents evaluated with optical coherence tomography. *Heart* 2008;**94**:566–70.
79. Choi H, Kim JS, Yoon D, Hong KS, Kim T, Kim B *et al.* Favorable neointimal coverage in everolimus-eluting stent at 9-months after stent implantation: comparison with sirolimus-eluting stent using optical coherence tomography. *Int J Cardiovasc Imaging* 2012 (Epub ahead of print).
80. Kim JS, Jang IK, Kim JS, Kim TH, Takano M, Kume T *et al.* Optical coherence tomography evaluation of zotarolimus-eluting stents at 9-month follow-up: comparison with sirolimus-eluting stents. *Heart* 2009;**95**:1907–12.
81. Kim JS, Kim JS, Kim TH, Fan C, Lee JM, Kim W *et al.* Comparison of neointimal coverage of sirolimus-eluting stents and paclitaxel-eluting stents using optical coherence tomography at 9 months after implantation. *Circ J* 2010;**74**:320–6.
82. Murakami D, Takano M, Yamamoto M, Inami S, Ohba T, Seino Y *et al.* Advanced neointimal growth is not associated with a low risk of in-stent thrombus. Optical coherence tomographic findings after first-generation drug-eluting stent implantation. *Circ J* 2009;**73**:1627–34.
83. Takano M, Inami S, Jang IK, Yamamoto M, Murakami D, Seimiya K *et al.* Evaluation by optical coherence tomography of neointimal coverage of sirolimus-eluting stent three months after implantation. *Am J Cardiol* 2007;**99**:1033–8.
84. Takano M, Yamamoto M, Inami S, Murakami D, Seimiya K, Ohba T *et al.* Long-term follow-up evaluation after sirolimus-eluting stent implantation by optical coherence tomography: do uncovered struts persist? *J Am Coll Cardiol* 2008;**51**: 968–9.
85. Tian F, Chen YD, Sun ZJ, Chen L, Yuan F, Song XT *et al.* Evaluation of neointimal coverage of overlapping sirolimus-eluting stents by optical coherence tomography. *Chin Med J (Engl)* 2009;**122**:670–4.
86. Gutiérrez-Chico JL, Räber L, Regar E, Okamura T, di Mario C, van Es GA *et al.* Tissue coverage and neointimal hyperplasia in overlap vs. non-overlap segments of drug-eluting stents 9–13 months after implantation: *in vivo*-assessment with optical coherence tomography. *JACC Cardiovasc Imaging* 2012 (under review).
87. Gonzalo N, Serruys PW, Okamura T, van Beusekom HM, Garcia-Garcia HM, van SG *et al.* Optical coherence tomography patterns of stent restenosis. *Am Heart J* 2009;**158**:284–93.
88. Takano M, Yamamoto M, Inami S, Murakami D, Ohba T, Seino Y *et al.* Appearance of Lipid-Laden intima and neovascularization after implantation of bare-metal stents: extended late-phase observation by intracoronary optical coherence tomography. *J Am Coll Cardiol* 2009;**55**:26–32.
89. Tanimoto S, Aoki J, Serruys PW, Regar E. Paclitaxel-eluting stent restenosis shows three-layer appearance by optical coherence tomography. *EuroIntervention* 2006;**1**:484.
90. Teramoto T, Ikeno F, Otake H, Lyons JK, van Beusekom HM, Fearon WF *et al.* Intriguing peri-strut low-intensity area detected by optical coherence tomography after coronary stent deployment. *Circ J* 2010;**74**:1257–9.
91. Nagai H, Ishibashi-Ueda H, Fujii K. Histology of highly echolucent regions in optical coherence tomography images from two patients with sirolimus-eluting stent restenosis. *Catheter Cardiovasc Interv* 2010;**75**:961–3.
92. Davlouros PA, Nikokiris G, Karantalis V, Mavronasiou E, Xanthopoulou I, Damelou A *et al.* Neointimal coverage and stent strut apposition six months after implantation of a paclitaxel eluting stent in acute coronary syndromes: An optical coherence tomography study. *Int J Cardiol* (in press).
93. Kim JS, Jang IK, Fan C, Kim TH, Kim JS, Park SM *et al.* Evaluation in 3 months duration of neointimal coverage after zotarolimus-eluting stent implantation by optical coherence tomography: the ENDEAVOR OCT trial. *JACC Cardiovasc Interv* 2009;**2**:1240–47.
94. Davlouros PA, Mavronasiou E, Xanthopoulou I, Karantalis V, Tsigkas G, Hahalis G, Alexopoulos D. An optical coherence tomography study of two new generation stents with biodegradable polymer carrier, eluting paclitaxel vs. biolimus-A9. *Int J Cardiol* (in press).
95. Windecker S, Serruys PW, Wandel S, Buszman P, Trznadel S, Linke A *et al.* Biolimus-eluting stent with biodegradable polymer versus sirolimus-eluting stent with durable polymer for coronary revascularisation (LEADERS): a randomised non-inferiority trial. *Lancet* 2008;**372**:1163–73.
96. Stone GW, Lansky AJ, Pocock SJ, Gersh BJ, Dangas G, Wong SC *et al.* Paclitaxel-Eluting Stents versus Bare-Metal Stents in Acute Myocardial Infarction. *New England Journal of Medicine* 2009;**360**:1946–59.
97. Serruys PW, Silber S, Garg S, van Geuns RJ, Richardt G, Buszman PE *et al.* Comparison of Zotarolimus-Eluting and Everolimus-Eluting Coronary Stents. *New Engl J Med* 2010;**363**:136–46.